A first 1415MHz survey with the Westerbork Synthesis Radio Telescope: an attempt to detect radio emission from quasi stellar objects

Katgert, P.; Katgert-Merkelijn, J.K.; Le Poole, R.S.; Laan, H. van der

Astron. & Astrophys. 23, 171 – 194 (1973)

A First 1415 MHz Survey with the Westerbork Synthesis Radio Telescope: An Attempt to Detect Radio Emission from Quasi Stellar Objects

P. Katgert, J. K. Katgert-Merkelijn, R. S. Le Poole and H. van der Laan
Sterrewacht Leiden

Received May 25, 1972

Summary. A survey has been carried out with the Westerbork Synthesis Radio Telescope in an attempt to detect radio emission from a sample of suspected QSO's. Due to the high sensitivity of the instrument, sources with flux densities down to ≈ 0.007 f.u. can be detected in a single twelve-hour observation; positional accuracy is of the order of an arcsecond.
Out of a total of 99 blue stellar objects, four are detected and another four may be radio emitting near the detection limit. Upper limits to the flux density are estimated for the remainder.
A catalogue of an additional 220 sources found in the survey is presented. An identification programme has been carried out for these sources, yielding 14 possible quasars (including three of the suspected QSO's), 25 galaxies and nine possible galaxies. Some of the identifications should be called cluster identifications, when there is a number of galaxies close to the radio source. It is suggested that in these cases the cluster medium gives rise to the radio emission, rather than the individual galaxies.
Source counts have been derived from a statistically unbiased sample: it is found that between 0.2 and 0.8 f.u. the number of sources *found* is a factor of two higher than was *expected* from an extrapolation of 1400 MHz source counts from other surveys covering a much larger area of the sky. Because possible systematic effects cannot account for the discrepancy, it is suggested that the excess must be explained by clustering on a scale of about 10 square degrees.
Below 0.1 f.u. the *differential* counts fall definitely below an extrapolation of the earlier 1400 MHz counts, the most likely value for the slope being between -1.8 and -2.1.

Key words: radio observations of QSO's – radio survey – identifications – source counts

I. Introduction

The Synthesis Radio Telescope at Westerbork, the Netherlands (hereafter referred to as the WSRT) began astronomical observations in June 1970. The systems-structure, its modes of operation, its performance and the data processing are described in the dissertation of Brouw (1971). Papers dealing with technical features of the instrument are in preparation by the engineering staff of the Netherlands Foundation for Radio Astronomy. For these reasons our instrumental description is extremely brief. The WSRT consists of twelve equatorially mounted paraboloids, each of 25 m diameter with a 8 mm mesh surface of 0.8 mm stainless steel wire. Telescopes 0, 1, 2, ..., 9 are fixed, 144 m apart, on an East-West line. Two movable telescopes, A and B, are on an East-West high precision track, 306 m long, beginning 27 m East of telescope 9.
The instrument is equipped with single frequency, dual polarization frontends. Each of the two dipoles in a fixed dish is combined with those in the movable dishes, to form 80 simultaneous interferometers for 20 simultaneous baselines. The operating frequency is 1415 MHz, the effective bandwidth 4 MHz, and the system noise temperature $\simeq 240°$ K.
The gain stability is better than 2%, the phase stability $\simeq 4°$, in the course of a week. The telescope is used as an earth rotation aperture synthesis instrument in the manner developed by Ryle and co-workers at Cambridge University. In this preliminary survey the observing mode was to track a point in the sky for twelve hours. The effective r.m.s. noise in such a 1×12^h observation is about 1.1 mf.u. (1 mf.u. = 1 milli flux unit $= 10^{-29}$ W m^{-2} Hz^{-1}). The synthesized beamwidth resulting from such an observation is about 22″ in RA and 22″ cosec δ in declination.
The effective field of view is determined by the single dish antenna pattern, which degrades the sensitivity by a factor of two at a radius of 0°.305. Since the twenty simultaneous spacings used do not provide a complete aperture sampling the synthesized sky maps contain not only source responses at the source location but

also elliptical grating rings for each point source response, of radius 10′ in RA and 10′ cosec δ in declination.

The chief astronomical motive of the programme was to attempt detection of a number of optically selected quasi-stellar objects and thus to extend our knowledge of the QSO radio luminosity function and of the relation between QSO's and QSS's (cf. Schmidt, 1970, for terminology).

Additional purposes this programme served may be summarized as follows:

1. To generate a sample of radio sources complete to $\simeq 10$ mf.u. in order to carry out preliminary source counts at this level.
2. To identify as much as possible of this sample of weak sources optically.
3. To test the system in its normal 1×12^h observing mode and to refine calibration procedures.
4. To gain experience in all phases of data processing and a variety of data representation and analysis.

These observations were largely carried out prior to October 1st 1970, the date of precise alignment of the orthogonal dipoles in the dishes. Observations after that date provide all Stokes parameters of the incident radiation. The results of this paper concern total intensity only. The experience gained in this programme is valuable for the analysis of the deep Westerbork 1415 MHz survey of the 5C 2 region carried out during 56 days early in 1971. This analysis is in progress.

II. Observations and Reduction

II.1. The Observations

For reasons made clear in the introduction we observed an optically well surveyed region, viz. the $6° \times 6°$ area centered on $\alpha = 13^h$, $\delta = +36°$. Braccesi obtained 48-inch Schmidt plates of this region in four colours. For a discussion of the optical data we refer to the original papers (Braccesi and Formiggini, 1969; Braccesi *et al.*, 1970). Here we only need to mention that these authors obtained a sample of suspected QSO's, selected on the basis of colours only, that is nominally complete to $b = 19.4$ with $(u-b)$-colours less than -0.35 (for the definition of the colour system we refer to Braccesi *et al.*, 1970). The sample contains 175 objects; for the brightest 31 objects redshifts have been obtained, thus confirming their quasi-stellar nature.

The radio survey of this region was carried out between the beginning of August 1970 and the end of October 1970. The survey consists of synthesis observations of eighteen fields, the positions of which were determined primarily by the distribution of QSO's over the area. The particular arrangement used permitted the observation of 99 objects within the 10 dB attenuation contour in the antenna pattern of the individual aerials; of these 99 objects 52 were within the -3 dB contour, including all those for which redshifts have been determined.

The pointing positions for the eighteen fields are given in columns 2 and 3 of Table 1. Column 4 of the same

Table 1. Description of the observations

No.	α (1950)	δ (1950)	(PA, PB)	UV-plane coverage		Map 1	Map 2	$\bar{S}_{low}$	$\bar{S}_{max}$	$\bar{S}_{min}$	N_1	$\bar{S}_{lim}$	N_2
1	$12^h45^m00^s$	37°45′	(90, 162)	−Tel 0	(−90°, +90°)	I	IV	18.5	81	5.85	13	6.75	11
2	12 46 00	34 45	(180, 252)	Complete		I	IV	13.5	106	6.10	17	7.0	14
3	12 48 30	33 45	(234, 306)	Complete		III	IV	32.0	361	6.65	10	10.0	6
4	12 53 30	35 45	(90, 162)	Complete		I, III	II, IV	27.5	135	6.30	17	9.0	14
5	12 54 00	35 25	(72, 144)	−Tel 0 −Tel 6	(−90°, − 9°) (−23°, −16°)	I	II	68.0	249	6.10	16	8.5	14
6	12 54 30	37 12	(72, 144)	−Tel 0 −Tel 0 −Tel 6 −Tel 9	(−90°, −56°) (+26°, +34°) (−90°, −31°) (−37°, −30°)	I, III	II, IV	125	510	6.85	18	9.5	14
7	12 58 20	36 53	(180, 252)	−Tel 5	(−90°, −80°)	III	IV	52.0	192	6.65	11	9.0	10
8	12 58 30	34 21	(180, 252)	Complete		III	IV	32.7	305	6.00	11	7.0	9
9	12 59 00	35 27	(180, 252)	−All interf	(−63°, −60°)	III	IV	18.0	85	6.65	17	7.75	10
10	13 01 00	32 23	(180, 252)	−Tel 4 −Tel B	(+ 8°, +19°) (−90°, −31°)	I	IV	18.0	49	6.85	11	10.0	7
11	13 01 40	35 53	(90, 162)	Complete		III	IV	37.0	315	8.50	13	8.5	13
12	13 01 40	37 42	(54, 126)	Complete		III	IV	18.5	161	6.75	10	6.75	10
13	13 04 40	36 38	(54, 126)	Complete		III	IV	21.0	93	6.50	17	7.75	13
14	13 05 00	37 25	(54, 126)	Complete		III	IV	15.0	30	6.00	14	7.25	12
15	13 05 20	34 58	(54, 126)	−Tel 0	(−90°, +90°)	III	IV	13.5	36	7.90	7	8.25	3
16	13 08 10	38 00	(54, 126)	Complete		III	IV	13.0	71	5.75	11	7.25	9
17	13 08 55	33 45	(180, 252)	−Tel 4 −Tel B	(−90°, −85°) (−90°, −88°)	I	IV	14.0	31	5.25	19	6.75	12
18	13 09 10	36 03	(180, 252)	−Tel B	(−31°, +81°)	I	IV	18.5	75	6.45	9	9.5	8

table contains the distances of telescopes A and B with respect to telescope 9 (distances are in meters). It is clear that the different observations are far from identical as regards the available baselines. The smallest baselines range from 260–1100 λ, the largest baselines from 6100–7600 λ. However the increment between consecutive baselines is 340 λ (72 m) in all observations.

Details about the coverage of the UV-plane are given in column 5 of Table 1. Nine of the eighteen observations are complete, i.e. they have been done with all twenty interferometers over the complete hour-angle range ($-90°$ to $+90°$). The observations of field 1 and 15 are also complete from the point of view of hour-angle coverage, but the largest two baselines (provided by telescope 0) have not been observed. In the seven remaining observations one or more telescopes are missing over certain parts of the hour-angle range.
The percentage of observations that are not complete is rather high. This is due to the fact that, although the WSRT became operational in June 1970, several parts of the system were at that time not yet working optimally. By the end of 1970, however, the reliability of the system as a whole had increased considerably.

II.2. Calibration

In order to be able to derive the sky brightness distribution from the complex visibility functions as measured by the different interferometers, one must have information about the following parameters: a) the lengths and orientations of the different baselines, b) the gain as well as the instrumental phase of the individual interferometer channels. These parameters were derived from observations, made regularly, of two calibrator sources: 3 C 48 and 3 C 295, the assumed positions and flux densities of which are:

	α (1950)	δ (1950)	S (1415 MHz)
3 C 48	$1^h34^m49^s.82$	32°54′20″.2	15.6 f.u.
3 C 295	$14^h\ 9^m33^s.44$	52°26′13″.6	21.8 f.u.

From the recorded amplitudes, gain corrections were derived which are estimated to be accurate to within 3%. Measurements of the linearity characteristics of the correlators indicate that this accuracy in gain correction is maintained over the whole range of flux densities concerned. From the hour-angle dependence of the recorded phases we derived corrections to the assumed baseline lengths and orientations, as well as the instrumental phases of all interferometer channels. The phases are estimated to be accurate to within four degrees, while the baselines are known to within two to four millimeters.
From the observations of 3 C 295 it became clear that this source is slightly resolved, the average visibility at the largest baselines ($\sim$7000 λ) being 0.96. This is consistent with observations at 410 MHz by Anderson and Donaldson (1967) which show 3 C 295 to have an angular extent of 4″.5 in position angle 143°. For this reason 3 C 295 was abandoned as a gain calibrator.

II.3. The Maps

Because a complete description of all available software has been given elsewhere (Brouw, 1971, and references contained therein), we will in the present context discuss only those steps in the processing of the data that are relevant to the source parameter extraction.
For all fields we made at least two fourier transforms, one directly from the observations and another in which the relatively stronger sources in each map were subtracted. In making the fourier transforms we did not treat all of the eighteen fields in the same way. More specifically, we used two types of grading function. The reason is that we wanted to get some insight into the effects of different weighting of the observations at different baselines, especially as regards the determination of angular extent of the sources. Information about the type of grading function is given in columns 6 and 7 of Table 1.
Maps of Types I and II have a gaussian grading function that is unity in the center of the UV-plane and 0.25 for the largest baseline present in the observation. Maps of the Types III and IV on the contrary have a grading function that is unity over the whole UV-plane. The main difference between the two types of map is that the synthesized beam patterns are different, such that for Types I and II the beam pattern is about 30% wider and has less pronounced near-in side lobes than for Types III and IV.
The dimensions of the synthesized maps generally were of the order of $1^\circ.4 \times 1^\circ.4$. Although at a distance of 0.7 degrees from the pointing position the sensitivity is degraded by a factor of 50, we made such large maps in order to minimize aliasing effects which are inherent in the fast fourier transform algorithm that was used (cf. Brouw, 1971). In all transforms the distance between adjacent synthesized intensities was chosen such that there were at least two intensities per synthesized half-power beam width both in right ascension and declination direction.
We already mentioned that we made at least two maps for each field.
In the second map (Types II or IV) the relatively stronger sources were subtracted, for which positions and flux densities had been determined from the first map. The map flux $\bar{S}$ (i.e. the real-sky flux density attenuated by the beam pattern of the individual interferometers) of the apparently weakest source that was subtracted is given in column 8 of Table 1. It should be mentioned here that two different procedures have been used for subtracting sources. Originally the subtraction was done in the following way. Given the

position of the source to be subtracted, its visibility at different baselines was derived from the observations by "phase-rotating" the observed signals to the source position and by subsequent averaging of the intensities so obtained. These intensities were then used to subtract the responses of the individual interferometers to the source from the observations.

This procedure has however two disadvantages. Firstly the derived intensities of the source at different baselines depend on the intensities of other sources in the map. Secondly an extended source is subtracted with different intensities at different baselines, so that it very often is impossible to determine from the remaining response in the subtracted map whether a source is extended or not. Therefore the option was provided to remove point sources by subtracting from the observations the response of a source with a specified flux density, having a visibility of unity at all baselines.

II.4. Source Parameter Extraction

For the determination of the positions and flux densities of sources use was made of a source finding program. This program essentially searches the map (or part of it) for intensities above a certain, specified intensity level. Thus a list is made of positions of possible sources. At these positions an iterative least squares fitting is done with the central part of the synthesized beam pattern, which is a by-product of the transform program. The beam pattern is used out to the second zero, i.e. including the first negative side lobe but excluding the grating ring responses. The flux density is determined by scaling the synthesized beam pattern to fit the observed intensities. Thus, local variations in the zero-level of the map are not accounted for. The program provides a list of the positions and flux densities of the "sources", as well as the mean errors in these quantities. Moreover, a "goodness of fit" parameter is given that is derived from the differences between the observed intensities and the scaled beam pattern.

The source finding program proved quite useful for sources that are sufficiently strong (having a signal to noise ratio of at least ten), but for the weaker sources the derived positions and flux densities may be affected rather strongly by the presence of grating ring responses. Unfortunately, the source finding program gives little information about angular extent because the "goodness of fit" parameter is not very sensitive to a slight broadening of the response to an extended source.

In addition to the source finding program we therefore also used contour plots, either of small regions around the stronger sources (maps I and III) or of the total map (maps II and IV). From the small contour plots, in which the declination scale was compressed so as to make the synthesized beam circular, we estimated the angular extent of the sources that were subtracted from the second map. From the large contour plots we estimated corrections to position and/or flux density of the weaker sources if such appeared necessary. Information about the angular extent of the weaker sources was also derived from the large contour plots. For those seven fields where the first and second map had been made with different grading functions we used the change in peak intensity from one map to the other as an additional indication of the extent of a source.

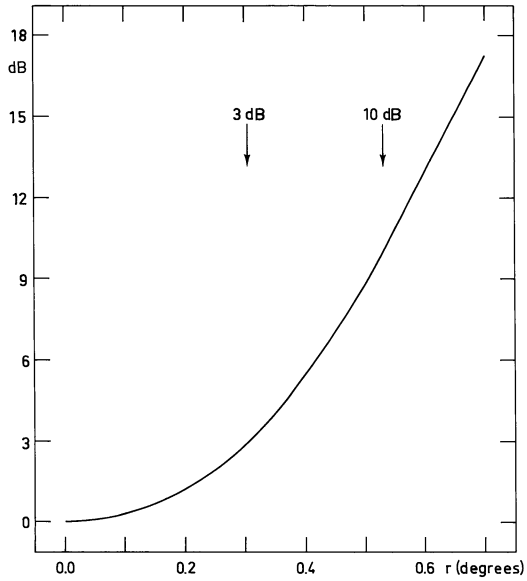

Fig. 1. The correction for the antenna pattern of the individual telescopes as a function of distance to the field center. The function is assumed to be axisymmetric

The map fluxes of the apparently strongest and weakest source detected in each field are given in columns 9 and 10 of Table 1 ($\overline{S}_{max}$ and $\overline{S}_{min}$); the number of sources with a map flux larger than or equal to $\overline{S}_{min}$ is given in column 11. Column 12 contains the limiting map flux down to which it was possible to define an essentially complete sample (cf. Section VI), while the number of sources above this limiting map flux is given in column 13. The real sky flux density of each detected source was computed from the map flux and a correction factor that accounts for the attenuation in the beam pattern of the individual telescopes. This correction was derived from those twenty sources that appear in two (overlapping) fields. From the differential attenuation for these sources we constructed the attenuation function that is given in Fig. 1. Out to 0°.3 the errors are estimated to be less than 5% (0.2 dB), including possible systematic errors. Between 0°.3 and 0°.7 errors may be as large as 10% (~0.4 dB).

II.5. Errors in Derived Source Parameters

a) Errors in Flux Density

From the error in the map flux, as given by the source finding program, we determined the actual error ($\Delta\overline{S}$) in the map flux (defining, roughly, the 70% confidence interval), taking into account extent and the presence of grating structure.

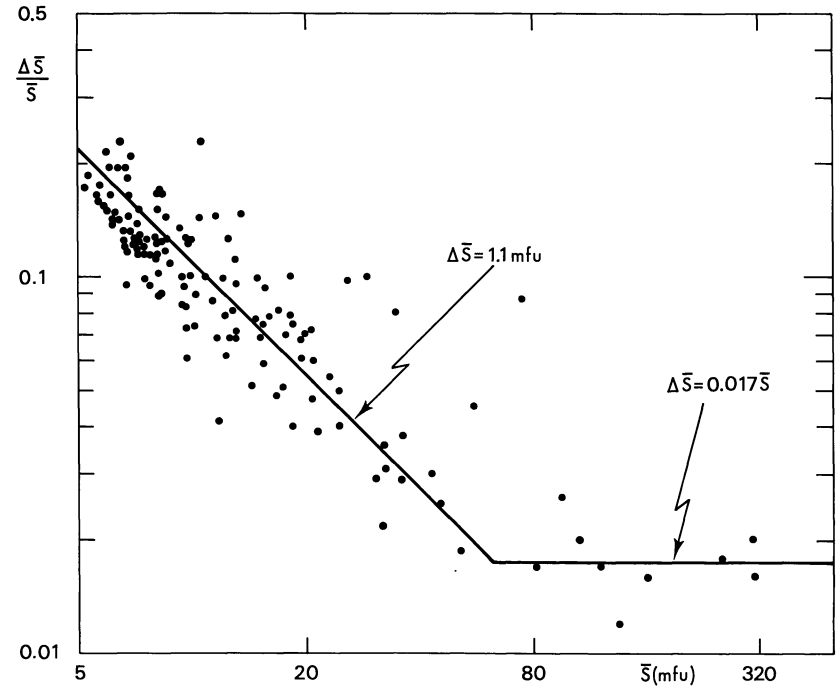

Fig. 2a. The ratio between quoted flux density error and flux density as a function of map flux for unresolved sources

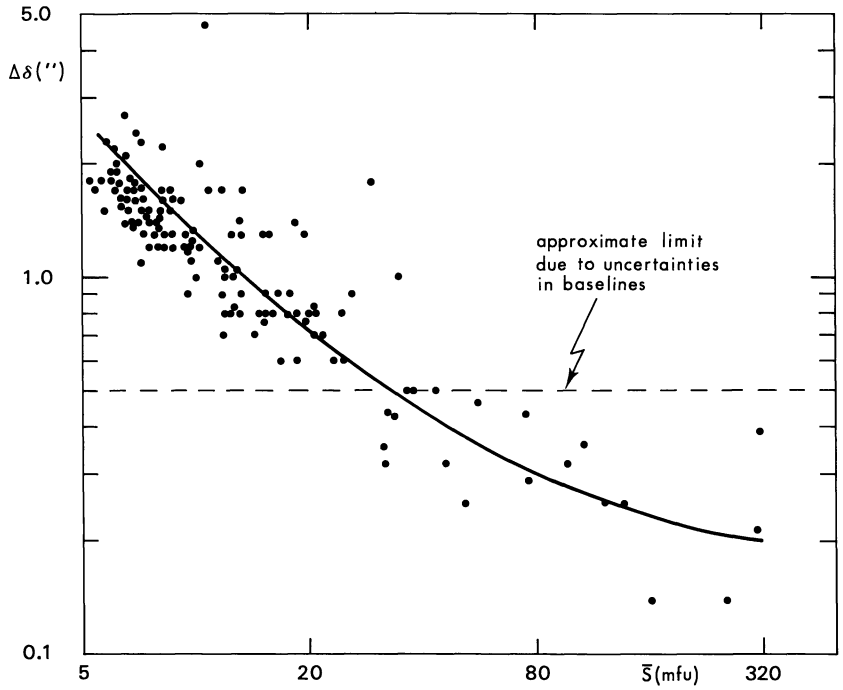

Fig. 2b. Quoted errors in declination as a function of map flux for unresolved sources

In Fig. 2a the ratio $\Delta\bar{S}/\bar{S}$ is shown as a function of map flux. Only sources with no detectable resolution for which the determination of flux density and position has not been affected by the presence of a grating ring response have been plotted. It appears that below $\bar{S}\simeq 65$ mf.u. $\Delta\bar{S}$ is roughly constant and, on the average, equal to 1.1 mf.u. which is consistent with the theoretical r.m.s. noise. It can be seen that all sources that were believed to be real have a signal to noise ratio of at least five (i.e. $\bar{S}>5.5$ mf.u.). Above $\bar{S}\simeq 65$ mf.u. $\Delta\bar{S}$ is roughly proportional to $\bar{S}$ and amounts to about 2%.

It should be realized that the flux density error quoted in the source list (Table 2) is equal to the error in the map flux multiplied by the attenuation correction. Possible errors in the attenuation function have not been included because they are not very accurately known.

b) Errors in Position

Figure 2b shows the quoted mean errors in declination as a function of map flux for the same sources that were used in Fig. 2a (the errors in right ascension are

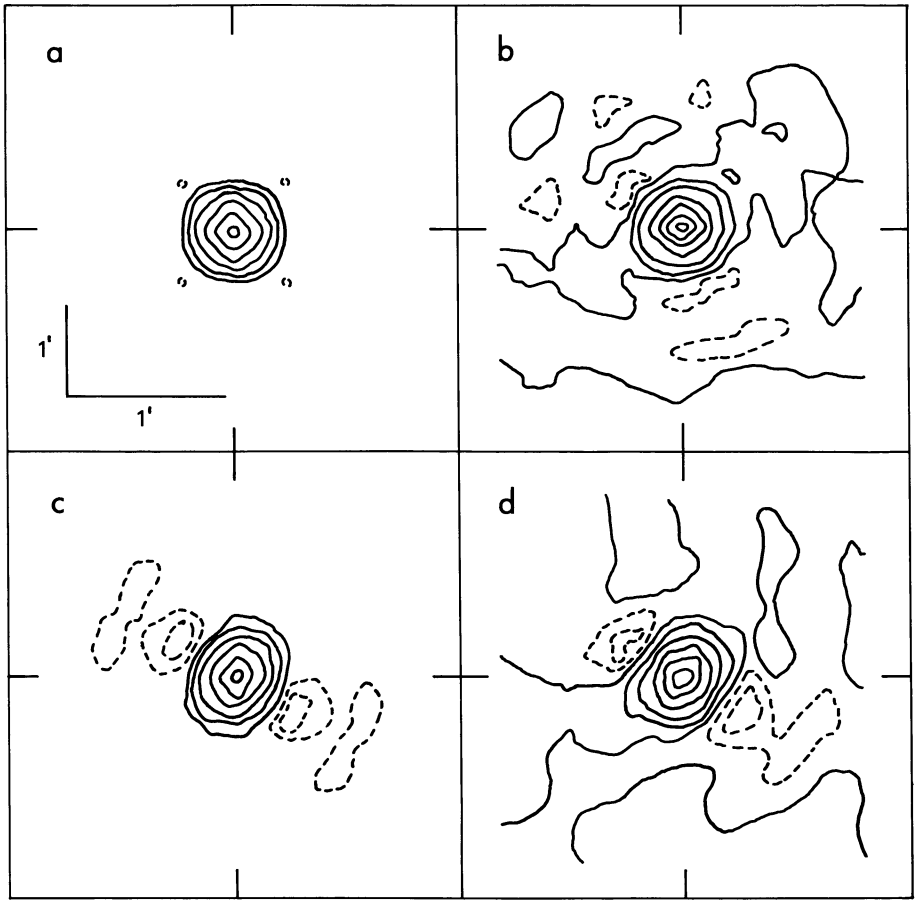

Fig. 3. Contour plots of synthesized beam patterns for fields 2(a) and 10(c), and of point sources in the same fields (b: 1245 + 34W3, d: 1259 + 32W1). Field 2 had complete UV-plane coverage, whereas in the observation of field 10 one of the moveable telescopes was missing over 60 degrees in hour angles (i.e. ten out of twenty interferometers)

smaller than those in declination by a factor of about 0.55). For the apparently weakest sources the errors in declination amount to some seconds of arc. The errors given in the source list are unrealistic for sources with $\overline{S} \gtrsim 30$ mf.u. because they are smaller than 0".5 which is the approximate limit imposed by the uncertainties in the baseline lengths and orientations.

c) Angular Extent

The procedure by which we determined the extent of a source has been described in Section II.4. When a source was considered to be resolved, we estimated the angular extent and the position angle of the major axis of the brightness distribution. The diameter Ψ given in the source list refers to the separation between the equal intensity components of a model double source. For sources that were clearly asymmetric we estimated the distance between the two unequal components. Of the five complex sources in the present list either a short description or a contour plot is given.

The uncertainty in Ψ is on the average 5–10". The accuracy of the diameters and position angles varies from field to field. In particular in fields 10 and 18 the accuracy is rather low. The reason for this can be seen from Fig. 3 where the computed synthesized beam patterns and the actual response to an unresolved source in fields 1 and 10 respectively are shown.

III. The Source List

Table 2 lists all sources found in the survey that are believed to be real. The source data were obtained as described in Section II.

Column 1. The source name. The sources have been named according to a modified Parkes system. The name consists of hours and minutes in right ascension, sign and degrees declination (both epoch 1950.0), an alphanumerical character denoting the observatory at which the source was observed (in this case W for Westerbork) and a running number of one or more digits. The sources are grouped in blocks of 1^m RA by 1° Dec., while inside these blocks they have been arranged in order of right ascension.

Columns 2 and 3 give the right ascension and declination (epoch 1950.0) with the position errors as derived from the errors given by the search programmes (cf. Section II.5).

Column 4. The flux density in mf.u. ($1 \text{ mf.u.} = 10^{-29} \text{ W m}^{-2} \text{ Hz}^{-1}$) together with the estimated mean error (cf. Section II.5). Corrections for any resolution and for primary-beam-pattern attenuation have been applied.

Column 5. The correction for attenuation due to the primary beam pattern.

Table 2

NAME	RA(1950)	DEC(1950)	S (MFU)	ATTEN	GR	STRUCTURE θ Ψ	IDENTIFICATION TYPE	OFFSETS		MAGN	REMARKS
1243+37W1	12 43 08.60	37 27 10.6	52.7	6.02	G	U					
	0.06	1.3	5.1								
1243+37W2	12 43 18.97	37 27 55.7	125	4.64		R 135 10"					
	0.05	0.9	17								
1243+38W1	12 43 37.45	38 08 22.2	72.2	6.12		U					
	0.04	0.7	3.1								
1244+34W1	12 44 35.42	34 58 01.5	24.2	2.76		P	GAL?	0.29F	1.4N	19.5	
	0.05	1.2	2.5								
1244+35W1	12 44 17.64	35 08 55.3	136	9.91	G	U					
	0.12	2.9	19								
1244+35W2	12 44 26.25	35 00 48.9	65.9	3.92		U	DB	0.0	7.2N	17.0	
	0.03	0.6	3.1								
1244+37W1	12 44 13.14	37 51 53.5	26.1	1.30		R 100 13"					
	0.06	1.3	6.0								
1244+37W2	12 44 17.14	37 31 44.9	133	1.64		U					
	0.01	0.3	2								
1244+37W3	12 44 25.38	37 52 35.7	11.3	1.24	G	P 40					
	0.09	1.7	2.0								
1244+37W4	12 44 25.76	37 26 51.9	40.9	2.19		U					
	0.04	0.8	1.6								
1244+37W5	12 44 47.83	37 52 00.0	6.6	1.13		U					
	0.11	2.3	1.0								
1245+34W1	12 45 10.46	34 27 09.6	27.0	2.46		P					
	0.05	1.1	2.6								
1245+34W2	12 45 21.09	34 55 28.7	21.3	1.41		U					
	0.06	1.3	1.5								
1245+34W3	12 45 23.39	34 21 32.4	405	3.81		U	GAL	0.17F	1.4N	19.0	
	0.02	0.4	8								
1245+34W4	12 45 33.31	34 55 10.5	27.1	1.30		U					
	0.04	0.8	1.3								
1245+35W1	12 45 22.40	35 00 46.4	11.7	1.88		U	GAL	0.0	9.4N	18.0	
	0.09	1.9	1.7								
1245+37W1	12 45 28.02	37 50 33.5	11.6	1.14		U					
	0.05	1.0	1.0								
1245+37W2	12 45 34.77	37 17 56.8	89.8	5.68		P 90					
	0.05	1.0	8.0								
1245+37W3	12 45 37.04	37 33 47.4	19.4	1.42	G	U					
	0.05	1.3	1.7								
1246+34W1	12 46 04.06	34 39 31.1	9.4	1.07		U					
	0.07	1.6	1.0								
1246+34W2	12 46 08.66	34 35 21.2	10.4	1.22		P	GAL	0.12F	4.3S	19.0	
	0.06	1.3	1.2								
1246+34W3	12 46 21.77	34 27 55.4	15.8	1.89		U					
	0.06	1.3	1.4								
1246+35W1	12 46 16.64	35 00 19.1	58.5	1.63		U					
	0.02	0.5	1.7								
1246+37W1	12 46 18.36	37 58 10.6	14.9	2.40		U					
	0.11	2.0	2.5								
1247+33W1	12 47 24.34	33 39 33.7	375	1.53	G	U	GAL?	0.41P	12.2S	20.0	4C33.30, B2
	0.02	0.5	15								

Table 2 (continued)

NAME	RA(1950)	DEC(1950)	S (MFU)	ATTEN	GR	STRUCTURE	Θ	Ψ	IDENTIFICATION TYPE	OFFSETS		MAGN	REMARKS
1247+33W2	12 47 30.02 0.01	33 39 48.9 0.2	517 20	1.43	G	U							4C33.30, B2
1247+33W3	12 47 37.49 0.04	33.59 50.3 1.0	20.4 1.5	2.02		U							
1247+33W4	12 47 47.52 0.36	33 30 25.2 7.2	22.5 5.4	1.80		R	70	15"					(1)
1247+33W5	12 47 51.44 0.04	33 38 41.5 0.9	19.0 1.4	1.24		U							
1247+34W1	12 47 12.26 0.03	34 35 35.8 0.7	40.9 1.6	1.88		U							
1247+34W2	12 47 19.23 0.06	34 24 28.1 1.4	31.2 3.0	4.59		U							
1247+35W1	12 47 42.12 0.07	35 05 31.6 1.6	68.5 6.9	6.85		P							
1247+37W1	12 47 19.42 0.07	37 57 33.1 1.4	55.1 7.0	7.82		U							
1248+33W1	12 48 23.49 0.06	33 41 32.7 1.3	9.8 1.0	1.03		U							
1248+33W2	12 48 31.10 0.07	33 44 47.0 1.6	6.6 0.8	1.00		U							
1248+34W1	12 48 22.24 0.08	34 56 17.1 1.7	55.7 7.8	9.14		U							
1248+35W1	12 48 09.49 0.03	35 00 13.9 0.7	340 21	8.26	G	U			GAL?	0.0	0.0	20.5	
1249+33W1	12 49 13.50 0.07	33 36 08.1 1.6	10.0 1.3	1.37		U							
1249+33W2	12 49 50.23 0.04	33 47 26.5 0.5	138 6	1.78	G	U							B2
1250+33W1	12 50 16.33 0.02	33 27 14.7 0.4	195 7	6.04		U			GAL?	0.24F	0.0	20.5	B2
1251+35W1	12 51 33.75 0.05	35 53 27.5 1.2	37.7 3.2	3.99		U							
1252+35W1	12 52 30.82 0.02	35 43 18.0 0.5	48.7 1.9	1.34		U							
1252+35W2	12 52 39.28 0.10	35 18 53.8 2.1	12.4 1.5	1.88		U							
1252+35W3	12 52 46.36 0.01	35 39 21.1 0.3	170 2	1.25		U							
1252+37W1	12 52 59.20 0.08	37 31 45.0 1.7	46.5 17.1	4.90	G	U							
1253+35W1	12 53 09.11 0.04	35 57 43.0 0.8	21.2 1.6	1.42		U							
1253+35W2	12 53 09.62 0.05	35 37 38.4 1.1	20.9 4.1	1.16	G	R	30	15"	GAL	0.48F	9.0N	17.0	
1253+35W3	12 53 14.29 0.04	35 13 01.6 0.9	71.1 15.0	1.58	G	R	105	15"	DB	0.17P	2.9S	16.5	SECOND GALAXY $0^{s}.6$F
1253+35W4	12 53 28.53 0.08	35 16 08.0 1.7	13.8 1.4	1.27		U							
1253+35W5	12 53 33.06 0.10	35 10 37.7 2.2	9.8 1.9	1.60		U							

Table 2 (continued)

NAME	RA(1950)	DEC(1950)	S (MFU)	ATTEN	GR	STRUCTURE Θ	STRUCTURE Ψ	IDENTIFICATION TYPE	IDENTIFICATION OFFSETS	MAGN	REMARKS
1253+35W6	12 53 33.15 0.03	35 29 31.4 0.6	23.7 1.8	1.12	G	U					
1253+35W7	12 53 43.06 0.03	35 41 00.9 0.7	15.2 0.8	1.06		U					
1253+35W8	12 53 46.90 0.05	35 54 22.8 0.9	17.7 1.5	1.23	G	P	90	DB	0.12P 3.2N	16.0	
1253+35W9	12 53 48.70 0.01	35 18 31.9 0.1	280 5	1.11		U					
1253+36W1	12 53 44.94 0.07	36 03 15.2 1.4	16.7 1.7	2.03	G	U		§			
1253+36W2	12 53 47.17 0.08	36 05 17.8 1.7	19.6 2.7	2.47	G	U		§			
1253+36W3	12 53 52.13	36 54 33.7	117 27	2.12		R		GAL §		20.5	
1253+36W3A	12 53 47.79 0.09	36 54 27.4 1.8	66.4 14.4	2.21		R	45 40"				D(135)=12"
1253+36W3B	12 53 58.73 0.24	36 54 43.1 4.3	33.2 8.0	2.01		R	90 35"				
1253+37W1	12 53 07.85	37 14 33.0	217 26	1.74		R	120	GAL §		20	SEE FIGURE 4A
1253+37W1A	12 53 04.24 0.07	37 14 59.9 1.5	78.3 10.1	1.84		R	120 20"				
1253+37W1B	12 53 11.46 0.07	37 14 06.0 1.5	107 16	1.64		R	135 30"				D(90)=30"
1253+37W2	12 53 08.83 0.10	37 19 22.8 2.2	15.7 2.4	1.91		U		§			
1253+37W3	12 53 14.77 0.08	37 15 42.6 1.7	18.9 2.8	1.60		U		§			
1253+37W4	12 53 40.47 0.08	37 31 10.7 1.7	18.6 3.1	2.72		U		§			
1253+37W5	12 53 55.94	37 29 55.1	679 86	2.15		R	15 45"				D(105)<6". COMPONENTS A & B: EQUAL DOUBLE. 4C37.35
1253+37W5A	12 53 55.22 0.10	37 29 34.4 2.2	263 52	2.10		U					
1253+37W5B	12 53 56.70 0.10	37 30 15.8 2.2	276 55	2.21		U					
1253+37W5C	12 53 55.94 0.07	37 29 55.1 1.8	140 43	2.15		U		§			
1254+35W1	12 54 15.54 0.04	35 40 58.8 0.9	36.2 4.3	1.23	G	U					
1254+35W2	12 54 20.66 0.07	35 23 32.1 1.5	11.0 2.1	1.05	G	U		DB	0.48P 10.8N	17.0	
1254+35W3	12 54 32.06 0.02	35 56 40.9 0.4	170 5	1.82		P	90				
1254+36W1	12 54 19.67 0.02	36 03 57.8 0.3	85.7 1.9	2.70		U					
1254+37W1	12 54 13.54 0.04	37 06 15.1 0.8	16.5 1.7	1.10		U		§			
1254+37W2	12 54 22.54 0.06	37 29 59.9 1.3	30.8 2.9	1.96		U		§			

Table 2 (continued)

NAME	RA(1950)	DEC(1950)	S (MFU)	ATTEN	GR	STRUCTURE Θ Ψ	IDENTIFICATION TYPE	OFFSETS	MAGN	REMARKS
1254+37W3	12 54 23.28 0.07	37 00 27.3 1.6	12.1 1.6	1.31		U	§			
1254+37W4	12 54 54.90 0.02	37 03 27.5 0.5	67.5 3.1	1.22		U	QSO	0.12F 2.9N	18.09	AB62
1254+37W5	12 54 57.27 0.05	37 12 59.5 1.0	18.8 2.7	1.07		R 165 10"	§			
1255+35W1	12 55 35.33 0.06	35 56 33.8 1.2	68.1 6.0	5.67	G	P 30	GAL	0.07F 1.8N	18.0	
1255+35W2	12 55 36.67 0.22	35 20 13.1 4.7	25.6 6.0	2.40		U				
1255+35W3	12 55 39.75 0.06	35 19 37.6 1.3	50.5 3.5	2.58		U				
1255+35W4	12 55 54.93 0.04	35 32 03.8 0.8	49.0 3.5	3.72		U				
1255+36W1	12 55 50.48 0.03	36 48 03.5 0.7	132 9.6	6.41		U				
1255+37W1	12 55 02.24 0.01	37 00 30.5 0.1	719 8	1.41		U	QSO?	0.05F 4.3N	18.5	4C36.22
1255+37W2	12 55 13.54 0.09	37 28 54.8 1.7	17.1 2.9	2.12		U	§			
1255+37W3	12 55 33.75 0.04	37 07 12.8 0.9	24.4 2.0	1.44		U	§			
1256+34W1	12 56 19.79 0.06	34 27 18.5 1.2	41.1 4.1	5.45		U				
1256+34W2	12 56 20.30 0.08	34 20 16.5 1.8	29.5 4.4	4.92		U	GAL?	0.05P 11.5S	18.5	
1256+35W1	12 56 05.71 0.03	35 52 58.5 0.7	204 15	11.15	G	U				
1256+35W2	12 56 37.30 0.05	35 29 04.1 1.1	48.4 6.0	6.68		U				
1256+35W3	12 56 49.26 0.04	35 36 05.0 0.8	116 8	5.82		U				
1256+36W1	12 56 44.64 0.02	36 48 06.7 0.3	433 23	2.26	G	U				
1256+37W1	12 56 06.23 0.05	37 15 10.4 0.9	102 12	2.21		R 45 15"				
1257+34W1	12 57 23.40 0.06	34 19 35.5 1.2	11.7 1.3	1.46		U	QSO?	0.19F 0.7N	19.0	
1257+34W2	12 57 31.74 0.01	34 13 01.3 0.2	460 9	1.51		U				
1257+34W3	12 57 44.91 0.08	34 32 22.6 1.8	14.9 1.9	1.53		P				
1257+34W4	12 57 45.80 0.06	34 24 25.5 1.2	11.6 1.1	1.21		U				
1257+35W1	12 57 25.68 0.07	35 16 00.2 1.5	21.1 2.5	2.90		U				
1257+35W2	12 57 48.40 0.06	35 31 25.7 1.3	19.8 2.5	1.58		U				
1257+36W1	12 57 08.52 0.36	36 33 14.4 7.2	240 56	3.70	G	R 120 30"				

Table 2 (continued)

NAME	RA(1950)	DEC(1950)	S (MFU)	ATTEN	GR	STRUCTURE	Θ	Ψ	IDENTIFICATION TYPE	OFFSETS		MAGN	REMARKS
1257+36W2	12 57 36.42	36 51 22.3	77.0	1.18	G	U							
	0.05	1.0	8.8										
1257+37W1	12 57 17.75	37 11 36.4	35.0	2.97		U			GAL?	0.24F	9.7S	20.5	
	0.04	0.9	2.4										
1257+37W2	12 57 36.72	37 06 07.1	121	1.64	G	U							
	0.02	0.4	4										
1258+34W1	12 58 22.02	34 32 29.0	10.2	1.31		U							
	0.06	1.3	1.0										
1258+34W2'	12 58 43.84	34 19 36.9	7.4	1.02		P							
	0.10	2.2	1.5										
1258+34W3	12 58 59.46	34 16 37.1	34.8	1.13		U			QSO?	0.12F	0.0	19.6	
	0.02	0.4	1.0										
1258+35W1	12 58 26.75	35 21 37.6	222	1.17		R							UNEQUAL DOUBLE (A & C) WITH BRIDGE (B)
			23										
1258+35W1A	12 58 25.28	35 21 43.8	99.5	1.18		U							
	0.08	1.8	11.8										
1258+35W1B	12 58 26.75	35 21 37.6	41.0	1.17		R							
	0.08	1.7	11.7										
1258+35W1C	12 58 27.85	35 21 22.3	81.9	1.17		U							
	0.08	1.8	11.7										
1258+35W2	12 58 39.30	35 49 03.0	238	2.99		R	165	40"					
	0.05	1.0	35										
1258+35W3	12 58 45.12	35 56 29.0	55.6	7.17	G	U							(1)
	0.12	4.3	7.2										
1258+35W4	12 58 57.60	35 35 11.0	11.7	1.15	G	U							
	0.06	1.4	1.7										
1259+31W1	12 59 27.58	31 53 46.3	244	17.27	G	U							B2
	0.06	1.3	24										
1259+32W1	12 59 40.41	32 22 40.3	76.5	1.77		U							B2
	0.02	0.5	2.3										
1259+33W1	12 59 07.08	33 53 07.4	77.8	6.49		U			QSO?	0.02F	1.1S	19.6	
	0.04	0.8	4.9										
1259+34W1	12 59 38.88	34 18 37.1	69.4	1.51		U							
	0.01	0.3	1.7										
1259+35W1	12 59 01.55	35 48 50.0	51.1	2.80		U							(1)
	0.17	3.6	4.1										
1259+35W2	12 59 13.85	35 24 03.7	7.0	1.04	G	U							
	0.08	1.8	1.5										
1259+35W3	12 59 45.30	35 12 45.7	20.5	1.79		U							
	0.05	1.1	1.8										
1259+35W4	12 59 49.02	35 12 11.2	18.4	1.93		U							
	0.06	1.2	1.5										
1259+36W1	12 59 19.98	36 56 01.3	14.2	1.35		P							
	0.07	1.4	3.4										
1259+37W1	12 59 04.78	37 14 16.2	45.2	3.20		P	75		DB	0.29P	0.7N	20.0	
	0.05	0.9	3.5										
1259+37W2	12 59 09.26	37 09 13.7	14.1	2.12		U							
	0.08	1.5	1.9										
1259+37W3	12 59 17.90	37 19 05.8	76.7	6.18		U							
	0.04	0.8	5.3										

Table 2 (continued)

NAME	RA(1950)	DEC(1950)	S (MFU)	ATTEN	GR	STRUCTURE	Θ	Ψ	IDENTIFICATION TYPE	OFFSETS		MAGN	REMARKS
1300+32W1	13 00 00.12 0.09	32 48 36.7 1.7	42.4 7.7	6.19		U							
1300+32W2	13 00 26.95 0.12	32 20 30.9 1.9	20.3 2.5	1.13	G	U							
1300+32W3	13 00 49.35 0.03	32 23 43.4 0.9	49.4 3.0	1.01	G	U			GAL	0.19F	1.4N	20.5	
1300+32W4	13 00 54.84	32 06 13.9	266 71	1.77		R	90	4'	GALS				D(0)=1'.5. SEE FIGURE 4B. B2
1300+32W4A	13 00 45.55 0.13	32 05 57.1 2.9	36.8 9.2	1.84		R							
1300+32W4B	13 00 53.06 0.09	32 05 57.8 2.5	117 32	1.81		R							
1300+32W4C	13 00 56.62 0.04	32 06 30.1 1.0	112 30	1.73		R							
1300+35W1	13 00 06.05 0.04	35 09 24.2 0.9	28.0 2.0	2.90		U							
1300+35W2	13 00 23.09 0.07	35 13 57.0 1.4	18.2 2.1	2.67		U							
1300+35W3	13 00 25.03 0.03	35 44 24.5 0.6	34.6 2.6	1.86		U							
1300+35W4	13 00 35.78 0.07	35 56 10.9 1.5	12.2 1.8	1.42		U			GAL	0.14P	0.7N	15.5	PECULIAR GALAXY
1300+35W5	13 00 53.57 0.03	35 56 12.6 0.8	19.5 1.5	1.22		U							
1300+36W1	13 00 33.58 0.02	36 06 16.2 0.3	255 4	2.11		U							
1301+32W1	13 01 01.68 0.06	32 28 52.9 1.1	14.6 1.5	1.08		P	60						
1301+32W2	13 01 24.67 0.04	32 22 47.5 0.8	13.8 1.1	1.07		U							
1301+32W3	13 01 35.85 0.08	32 34 18.6 2.0	14.9 2.2	1.44		U							
1301+35W1	13 01 32.77 0.01	35 25 54.7 0.3	492 13	5.12		U							
1301+36W1	13 01 26.10 0.05	36 05 35.8 1.1	13.6 0.8	1.39		U							
1301+37W1	13 01 23.64 0.07	37 51 31.2 1.4	9.7 1.5	1.23	G	U			QSO?	0.19P	4.3S	18.0	
1301+37W2	13 01 33.86 0.08	37 44 57.1 1.6	8.4 1.0	1.03		U							
1301+37W3	13 01 47.56 0.01	37 25 12.7 0.1	286 4	1.78		U							
1301+37W4	13 01 49.18 0.06	37 56 43.4 1.2	12.7 1.3	1.54		U							
1301+37W5	13 01 58.92 0.07	37 58 01.8 1.4	11.8 1.7	1.72		U							
1301+38W1	13 01 24.54 0.06	38 12 15.1 1.2	800 120	8.01		R	45	20"	DB	0.19F	1.4N	19.5	POSSIBLY EQUAL DOUBLE, SEPARATION=18". 4C38.35
1301+38W2	13 01 55.41 0.01	38 03 38.7 0.3	146 3	2.81		U			GAL	0.05F	2.2S	>20.5	

Table 2 (continued)

NAME	RA(1950)	DEC(1950)	S (MFU)	ATTEN	GR	STRUCTURE Θ Ψ	IDENTIFICATION TYPE	OFFSETS	MAGN	REMARKS
1302+32W1	13 02 11.38 0.06	32 22 33.9 1.2	13.6 2.0	1.57		U	QSO?	0.14F 10.4N	19.02	AB114
1302+32W2	13 02 17.12 0.08	32 29 37.8 1.7	16.2 2.3	1.88		U				
1302+35W1	13 02 13.77 0.04	35 39 36.9 0.4	489 8	1.56		U				
1302+35W2	13 02 17.59 0.05	35 55 57.0 1.0	20.2 3.5	1.15		R 75 12"				
1302+35W3	13 02 58.84 0.05	35 15 41.1 1.0	169 13	13.76		U	§			
1302+36W1	13 02 38.73 0.06	36 09 22.0 1.3	31.6 6.6	2.38		R 300 18"				
1302+36W2	13 02 53.08 0.06	36 23 37.7 1.0	143 22	4.39		R 165 50"				D(75)=10"
1302+37W1	13 02 32.18 0.07	37 49 06.6 1.4	24.8 2.5	1.36		U				
1302+37W2	13 02 49.73 0.02	37 28 14.4 0.5	94.4 6.7	2.22		P 90				
1303+34W1	13 03 44.57 0.07	34 49 27.8 1.5	21.6 2.7	2.66		U				
1303+35W1	13 03 54.05 0.04	35 46 07.5 0.9	75.0 8.3	5.75		U	GAL	0.0 0.0	19.0	
1303+36W1	13 03 01.11 0.06	36 07 34.8 1.2	184 35	2.83		R 10 72"				
1303+36W2	13 03 17.90 0.03	36 33 35.2 0.6	44.8 2.3	1.81		U				
1303+36W3	13 03 31.82 0.04	36 38 57.7 0.7	217 36	1.45		R 165 1'	GAL	0.19F 1.4S	19.0	
1303+36W4	13 03 31.96 0.05	36 55 33.6 2.5	126 10	2.93	G	U	GAL	0.19F 1.8S	18.5	GALAXY IN CLUSTER
1303+36W5	13 03 36.49 0.05	36 09 22.1 1.0	66.3 7.9	6.28		P 120				
1303+36W6	13 03 59.27 0.08	36 47 55.0 1.4	69.3 13.9	1.39		R 150 15"				
1303+37W1	13 03 12.56 0.06	37 51 53.4 1.2	32.7 5.2	2.51		R 30 10"				
1303+37W2	13 03 35.84 0.05	37 00 07.3 0.8	122 9	4.26		P 150				
1304+35W1	13 04 01.55 0.07	35 26 02.8 1.4	84.2 9.6	10.66		U				
1304+36W1	13 04 00.29 0.10	36 46 49.3 1.8	39.0 3.9	1.32		U	QSO?	0.05F 4.3N	20.0	
1304+36W2	13 04 01.33 0.05	36 23 56.0 1.0	26.6 2.1	1.68	G	U				
1304+36W3	13 04 03.27 0.14	36 59 28.5 2.4	21.5 4.6	3.08		U				
1304+36W4	13 04 04.34 0.15	36 58 26.5 2.7	17.9 4.1	2.76		U	GAL	0.12F 2.9N	19.5	
1304+36W5	13 04 26.12 0.02	36 29 31.0 0.4	38.4 1.2	1.18		U				

Table 2 (continued)

NAME	RA(1950)	DEC(1950)	S (MFU)	ATTEN	GR	STRUCTURE Θ	Ψ	IDENTIFICATION TYPE	OFFSETS		MAGN	REMARKS
1304+37W1	13 04 02.81 0.09	37 42 42.6 1.6	18.0 2.2	2.57		U						
1304+37W2	13 04 51.06 0.10	37 12 28.7 1.8	14.1 4.1	1.37		R	30 25"	GAL?	0.36F	0.7S	20.5	
1305+34W1	13 05 27.61 0.07	34 59 10.3 1.7	13.6 2.0	1.01		U						
1305+36W1	13 05 07.17 0.07	36 47 18.9 1.3	18.7 1.9	1.26	G	U						
1305+36W2	13 05 07.58 0.04	36 55 16.9 0.8	41.3 2.5	1.97		U		GAL?	0.24F	0.7S	20.5	
1305+36W3	13 05 22.16 0.12	36 11 34.3 2.3	40.5 6.1	5.55		U						
1305+36W4	13 05 28.23 0.06	36 18 37.8 1.2	30.2 3.7	2.74		P	30					
1305+37W1	13 05 23.70 0.07	37 52 56.0 1.4	45.4 5.7	5.98		U						
1305+37W2	13 05 24.15 0.08	37 11 42.1 1.5	11.1 1.3	1.48		U						
1305+37W3	13 05 29.96 0.05	37 18 16.0 0.9	21.1 1.5	1.18		U						
1305+37W4	13 05 32.99 0.10	37 48 28.2 1.9	22.1 4.6	3.68		U						
1305+37W5	13 05 36.82 0.04	37 20 42.6 0.8	17.7 1.0	1.16		U						
1305+37W6	13 05 43.10 0.07	37 44 27.8 1.3	22.7 2.9	2.63		U		§				
1305+37W7	13 05 48.87 0.04	37 15 08.8 0.8	28.5 1.7	1.46		U						
1306+33W1	13 06 56.31 0.08	33 46 43.3 1.8	20.2 3.5	3.85		U		QSO?	0.24F	5.0N	19.4	
1306+35W1	13 06 08.00 0.02	35 10 03.8 0.5	68.7 3.6	1.62		R	30 10"	GAL?	0.84F	0.7S	19.0	
1306+36W1	13 06 02.58 0.10	36 37 33.3 1.8	12.0 2.6	1.74	G	U						
1306+36W2	13 06 46.41 0.09	36 52 51.2 1.5	141 24	6.89		R	120 30"	GALS				CLUSTER. SEE FIGURE 4C.
1306+38W1	13 06 47.77 0.07	38 23 40.6 1.3	46.5 5.6	6.28		U		GAL §	0.0	0.0	19.0	
1307+33W1	13 07 11.68 0.08	33 32 03.9 1.8	22.7 3.6	4.01		U						
1307+33W2	13 07 24.30 0.06	33 27 11.4 1.4	33.6 4.0	4.45		U						
1307+34W1	13 07 15.63 0.06	34 13 41.8 1.4	144 16	17.77		U						
1307+34W2	13 07 44.12 0.05	34 19 01.5 1.0	482 36	24.09	G	U						
1307+34W3	13 07 56.33 0.07	34 00 15.5 1.6	14.2 2.0	2.23		U		QSO?	0.29F	2.9N	18.0	
1307+35W1	13 07 03.61 0.08	35 54 19.4 1.1	93.2 8.4	5.06	G	U						

Table 2 (continued)

NAME	RA(1950)	DEC(1950)	S (MFU)	ATTEN	GR	STRUCTURE Θ	Ψ	IDENTIFICATION TYPE	OFFSETS		MAGN	REMARKS
1307+35W2	13 07 04.93	35 03 35.7	23.3	2.92		U						
	0.06	1.3	2.9									
1307+35W3	13 07 21.03	35 04 53.4	37.9	4.33		P 15		QSO?	0.36P	2.9N	19.0	
	0.09	1.8	4.3									
1307+35W4	13 07 55.20	35 55 23.5	11.5	1.79		U						
	0.10	1.6	2.2									
1307+37W1	13 07 15.87	37 39 21.1	408	3.26		R 165	1'	GALS §			19.0	D(330)=25" TRIPLE?
	0.05	1.0	65									SEE FIGURE 4D. 4C37.36
1307+37W2	13 07 46.71	37 44 50.3	15.7	1.65		P 90		GAL	0.14P	2.9N	17.0	
	0.08	1.4	2.1									
1307+37W3	13 07 51.06	37 56 39.6	13.8	1.06		U						
	0.05	1.0	1.0									
1307+37W4	13 07 54.41	37 48 01.5	46.6	1.35		U						
	0.06	1.0	3.7									
1307+37W5	13 07 59.27	37 41 19.8	12.0	2.08		U						
	0.08	1.5	2.1									
1308+33W1	13 08 09.75	33 36 09.1	24.4	1.39		U						
	0.03	0.8	1.2									
1308+33W2	13 08 14.98	33 47 44.1	33.5	1.17	G	U						
	0.03	0.8	2.3									
1308+33W3	13 08 18.57	33 39 03.9	19.4	1.21		R 135	10"	QSO?	0.53F	9.4N	19.24	AB153
	0.06	1.3	2.4									
1308+33W4	13 08 27.71	33 33 45.1	8.4	1.37		U						
	0.07	1.7	1.2									
1308+33W5	13 08 59.07	33 21 36.6	82.1	3.32		U						
	0.04	0.8	3.3									
1308+34W1	13 08 02.29	34 01 59.1	46.3	2.38	G	U						
	0.04	0.9	2.4									
1308+35W1	13 08 16.80	35 42 08.1	243	3.35		R 105	15"					
	0.04	0.6	34									
1308+35W2	13 08 25.27	35 41 02.3	33.8	3.45		U						
	0.07	1.2	4.1									
1308+36W1	13 08 56.55	36 13 09.3	93.8	1.25		U		QSO?	0.14F	4.3N	20.0	
	0.03	0.4	8.1									
1308+37W1	13 08 06.28	37 50 51.8	11.8	1.19		U						
	0.07	1.3	1.2									
1308+37W2	13 08 40.89	37 37 54.5	22.6	3.14		U						
	0.09	1.7	3.1									
1308+38W1	13 08 01.83	38 27 27.3	70.5	5.39		U		§				
	0.07	1.4	6.7									
1308+38W2	13 08 30.33	38 13 53.1	18.1	1.51		U						
	0.05	1.0	1.8									
1309+33W1	13 09 18.42	33 08 35.5	152	22.78		U		QSO?	0.0	4.3N	18.0	UV VARIABLE?
	0.08	1.8	30									
1309+33W2	13 09 21.50	33 36 45.1	6.5	1.22		U						
	0.07	1.7	1.2									
1309+33W3	13 09 38.29	33 31 04.7	53.9	1.74	G	U						
	0.02	0.5	2.2									
1309+33W4	13 09 42.56	33 42 20.3	17.9	1.24		P						
	0.05	1.1	2.2									

Table 2 (continued)

NAME	RA(1950)	DEC(1950)	S (MFU)	ATTEN	GR	STRUCTURE Θ	STRUCTURE Ψ	IDENTIFICATION TYPE	IDENTIFICATION OFFSETS	MAGN	REMARKS
1309+35W1	13 09 10.10	35 43 49.2	49.6	2.16		U					
	0.04	0.6	2.7								
1309+36W1	13 09 53.99	36 29 08.2	104	5.45		P	240				
	0.05	0.8	12								
1309+38W1	13 09 15.36	38 08 41.4	22.7	1.61	G	U					
	0.05	1.0	2.0								
1310+33W1	13 10 04.20	33 53 13.7	52.1	1.74		P	30				
	0.03	0.6	3.5								
1310+33W2	13 10 04.97	33 26 07.8	19.5	3.48		U		§			(1)
	0.11	2.3	3.1								
1310+35W1	13 10 14.51	35 56 34.0	15.2	1.52		U					
	0.08	1.2	1.9								
1310+36W1	13 10 58.75	36 17 16.9	118	4.57		U					
	0.06	0.9	11								
1311+33W1	13 11 27.57	33 27 48.1	140	20.48		U					B2
	0.07	1.7	18								

(1) FLUX DENSITY AND POSITION DETERMINED FROM LARGE CONTOUR MAP.

Column 6. The presence of a G in this column indicates that the position and/or flux determination is affected by the presence of grating rings.
Column 7. Information on resolution as follows: U = no detectable resolution, P = possibly resolved, R = resolved.
Columns 8 and 9 give further information on resolution: If column 7 contains a P and if the map flux is at least 10 mf.u., a position angle is given (r.m.s. = ±15°); if column 7 contains an R the position angle (r.m.s. = ±7.5°) and angular extent are given. A position angle >180° indicates asymmetry. If a source is resolved in two directions further information is given in column 15.
Column 10. Type of identification.
Column 11. A paragraph sign indicates that the identification was done on the Palomar Sky Survey prints, using overlays (cf. Section IV.1).
Columns 12 and 13. Displacement of the optical position from the radio position. The r.m.s. error in the optical position is of the order of two arcseconds.
Column 14. The magnitude of the identified objects. For galaxies these have been estimated from the E-prints of the Palomar Sky Survey; for suspected QSO's from the O-prints. The r.m.s. error in the estimated magnitudes is approximately 1^m; the magnitudes for the AB objects have been taken from Braccesi *et al.* (1970).
Column 15. Remarks.

IV. The Identifications

IV.1. The Identification Procedure

The sources in the present catalogue form the first extensive sample of very weak sources with accurate radio positions at 1415 MHz (position errors are generally of the order of an arcsecond). There is the advantage that a good optical counterpart exists (per definition) in the form of a number of full field 48″ Schmidt plates in four colours (*IR*, *V*, *B*, *U*) taken by Braccesi and used for the search for those *UV*-excess objects which we attempted to detect in the present programme (Braccesi *et al.*, 1970).
It therefore seemed worthwhile to invert the programme and try to optically identify the sources listed in Table 2 from these plates. The identifications were made at Bologna with the aid of a $X-Y$ measuring machine with which we measured positions accurate to about 2″.

The method used was the following:
Two stars were used as reference stars to secure proper orientation of the plates at each measuring session; about 25 comparison stars with known positions were measured to determine the plate constants. Plate coordinates were then computed for each of the sources in the catalogue (programme by Formiggini). The blue plate was inspected at the position of each source and the presence of objects near enough (generally within about 5″) to the crosswires noted. Next, a comparison was made with the ultraviolet plate. This was greatly facilitated by a special feature of the instrument, namely the possibility to project the images of one plate onto the other plate. In this way it proved to be very easy to decide whether an object had a marked *UV* excess.
The third step was to inspect the infrared plate in the same way; at this stage a number of galaxies were found that did not appear on the first two plates. As a fourth

step a comparison was made between the B and the V plate, to check on any objects that might have a pronounced blue-excess, even though no UV excess had been found.

The identifications are entered in Table 2.

For a number of sources identifications have not been attempted in this way, either because they lay outside the plates or because no radio positions were known at the time. For these sources an attempt at identification was made at a later time by the usual and well-known method of plotting an overlay with the positions of the source and of a number of comparison stars and then inspecting the Palomar Sky Survey prints in the position of the source. Due to the much larger inaccuracy intrinsic in this method these identifications will generally be less reliable (errors typically of the order of 10″). Sources for which this method was followed are indicated by a paragraph sign in column 11 of Table 2.

IV.2. Identification Results and Comments on Catalogue Entries

Most of the galaxy identifications are fairly standard; 34 sources could be identified with galaxies. Some of the galaxies look peculiar; these will be discussed later on.

From the QSO identifications however, we can get some indication about the completeness of the list given by Braccesi *et al.* and about the existence of optically faint QSO's. Table 3 lists the QSO's found, grouped according to which "Braccesi-criteria" they do or do not fulfil.

One QSO identification is not entered in the table, this is 1309 + 33 W 1 ($m_b \sim 18$), for which $u-b$ was found to be > -0.35 on the plate which Braccesi *et al.* used for their search but which showed a much more pronounced UV excess on the U and B plates used for the identification work. As the plates were taken at different epochs, this clearly indicates that the object is variable, most probably in the ultraviolet.

One other blue object, which seemed interesting, had to be discarded: it is the object which lies near to the complex source 1253 + 37 W 1. The identification was made with the aid of an overlay on the Palomar Sky Survey prints but should be sufficiently reliable. An enlargement of the region is given in Fig. 4a, with the radio contours drawn in. The centroid of the radio emission coincides with a 20^m galaxy; to the north of the galaxy lies a blue ($18^m.5$) object which seems to have a jet in the direction of the galaxy. It was first thought that this might indicate a physical connection; however, a spectrum of the object shows it to be a galactic star (Schmidt, private communication). The "jet" is therefore more likely to be a faint galaxy, the more so as it appears more strongly on the infrared plate.

A few other interesting objects should be mentioned.

Table 3. Optical properties of the identified QSS's

	$u-b < -0.35$	$u-b > -0.35$
$m_b < 19.4$	1254 + 37 W 4 = AB 62	1257 + 34 W 1
	1255 + 37 W 1	1301 + 37 W 1
	1302 + 32 W 1 = AB 114	1306 + 33 W 1
	1307 + 34 W 3	
	1307 + 35 W 3	
	1308 + 33 W 3 = AB 153	
$m_b > 19.4$	1258 + 34 W 3	1308 + 36 W 1
	1259 + 33 W 1	
	1304 + 36 W 1	

The complex 1300 + 32 W 4 (Fig. 4b), coinciding with a cluster of galaxies. No certain identifications of any of the sources in the complex or of its center of gravity with individual galaxies could be made (there is a galaxy quite near to the center of gravity but we feel that identification with this galaxy, which is one of the fainter galaxies in the cluster, is unlikely). Still, we get the impression that the two are definitely related. A high-resolution radio map might give further information.

The identification of 1306 + 36 W 2 (Fig. 4c) is in some respects similar to the previous case; this source is fairly extended but could not be resolved into separate components. Four galaxies lie within the region of the radio emission so no single identification could be made.

About three faint galaxies ($\sim 19^m$) lie within the radio contours of 1307 + 37 W 1 (Fig. 4d). In this case the central galaxy lies near to the peak of the radio emission but we cannot exclude the possibility that the other two galaxies are related to the complex.

Apart from these complexes a few peculiar galaxies were found. The best example is 1300 + 35 W 4, which is identified with a fairly red $15^m.5$ galaxy which has an extremely blue extension. On Braccesi's plates the extension looks like an arm; on the Palomar "E" print it looks more like a ring.

A few qualitative conclusions may be drawn from the identification content of the sample.

1) A marked UV excess is probably not a very necessary requirement for an object to be quasi-stellar. The objects with little if any UV excess that coincide with radio sources are, in our view, very likely to be quasars, because of this very positional coincidence. The interesting possibility arises that, though there are various other ranges of z where quasars have comparatively small UV excesses, ($z = 0.5 - 1.0, \sim 1.7, \sim 2.2$), some of these objects might be the high-redshift ($z > 2.5$ or so) objects that are so avidly (and with so little success) sought.

2) The possibility cannot be excluded that there are clusters of galaxies in which the intergalactic cluster medium emits far more radio radiation that the individual cluster members (Figs. 4b, c, d).

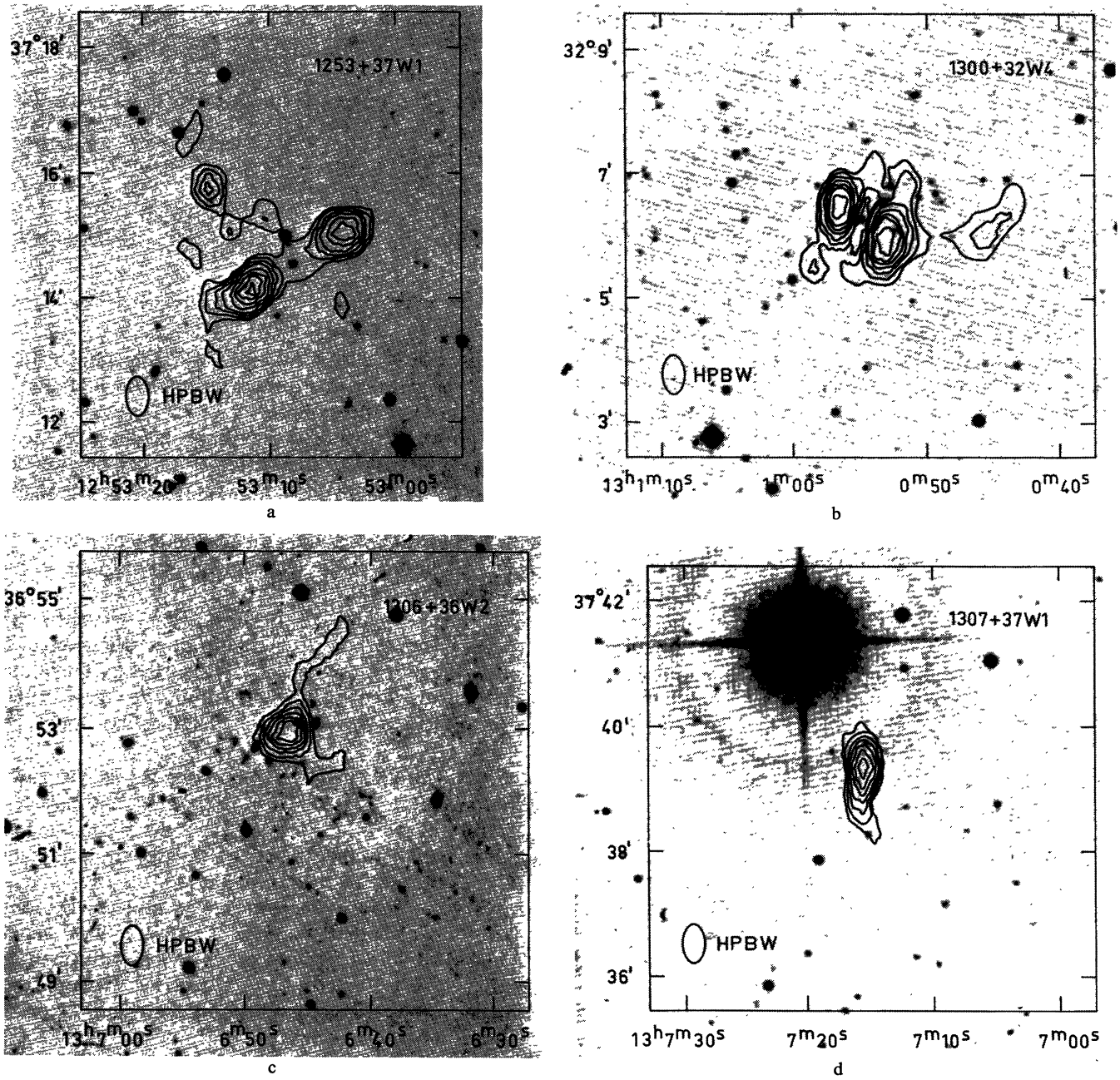

Fig. 4. Radio contour plots superimposed on enlargements of the Palomar Sky Survey "E" prints for four interesting identifications. Zero contours are not included; lowest contours included are still heavily affected by noise (about 2σ). Photographs courtesy of the National Geographic Society

Additional support for this conclusion can be obtained from the results of the resolution statistics: Table 4 gives the distribution of identifications over the different resolution classes (*R*, *P*, and *U*) for the 126 sources with a mapflux in excess of 10 mf.u. in 16 of the fields: sources from fields 10 and 18 are excluded because of the difficulty in estimating resolution (cf. Section II.5). Inspection of the table shows that there is a significant difference in the galaxy identification content between resolved and unresolved sources. Of the former class, a surprising 40% could be identified with galaxies. This very interesting effect can easily be explained if one considers that without exception "cluster identifications" are with resolved sources and are included under galaxy identifications. Although there are only

Table 4. Radio structure versus identification type

	NI	G	QS
R	15	10	1
P	11	3	0
U	70	11	5

two of these in the present sample, inspection of the plates shows that near the positions of at least two more resolved sources there is evidence of clustering (1253 + 35 W 2, 1253 + 37 W 1).

The identifications were made without knowledge of resolution characteristics, but we relaxed our position criteria somewhat for the resolved sources when information on resolution became available. Thus a few galaxies that were disregarded in the first instance were later included as they fell well within the "radio contours" (1306 + 35 W 1 is a good example). Of course, the number of chance coincidences will be increased somewhat by this procedure. Considering that the diameter of the field of search has been increased, on the average, from 10″ to 25″ and assuming 2000 galaxies per square degree brighter than magnitude 20.5 (on the PSS E-print) we expect 10% chance coincidences (or one object).

V. The Detection of the Blue Stellar Objects

V.1. The List of Blue Objects

Table 5 lists those objects from Braccesi's list that we observed in the present programme, as follows.

Column 1. Name in the list of Braccesi *et al.* AB numbers are not to be confused with the B numbers of Braccesi, Lynds and Sandage (1968).
Columns 2 and 3. Right ascension and declination (both epoch 1950.0).
Column 4. Flux density or upper limit to the flux density.
Column 5. Estimated error in the flux density of the detected sources.
Column 6. The correction for the attenuation due to the primary beam pattern.
Column 7. Redshift.
Column 8. Frequency of emission in MHz corresponding to the observing frequency of 1415 MHz.
Column 9. LogP_{emitted} in W Hz^{-1} (upper limits are given for those sources with known z that were not detected).
Column 10. Remarks, such as data on offsets in the case of detection, reliability of the detection etc.

V.2. The Detection Procedure

Contour maps were made for all Braccesi-objects in the observed fields. The interval between successive contours was 1.5 mf.u. (map flux). Upper limits (and, occasionally, flux densities for the possible detections) were determined from the contour maps; the upper limits were, of course, strongly dependent on local noise levels and any grating structure present. In the absence of such structure they were generally taken to be equal to 2.5 m.f.u. ($\sim 2.5\,\sigma$). For non-detected objects that were observed in two fields, the lowest of the two upper limits has been entered in Table 5.

In Fig. 5 upper limits to the emitted radio luminosity are plotted against the emission frequency for all objects with known redshift. The full-drawn line corresponds to a detection limit of 8 mf.u. Detections are indicated by circles, possible detections by crosses. It

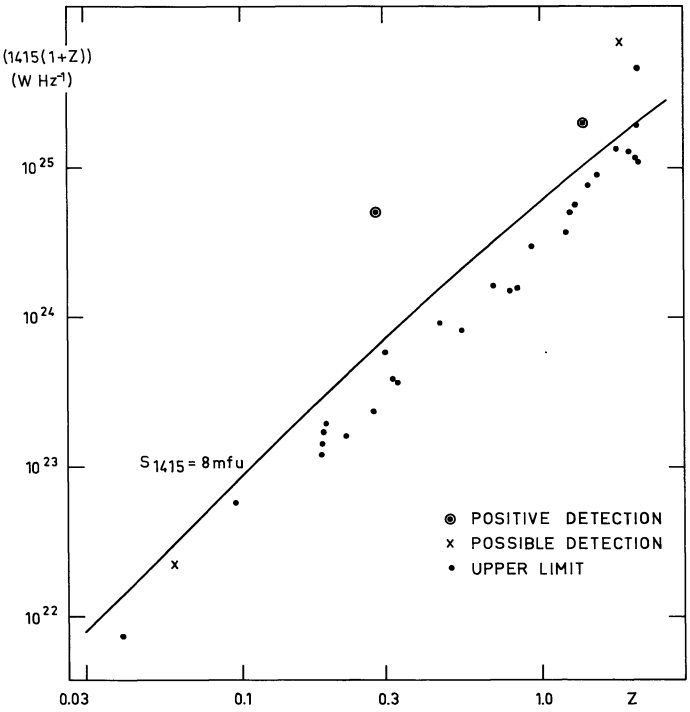

Fig. 5. Values of logP_{emitted}, or the upper limit to such values, as a function of redshift for the 31 AB objects with known redshift ($q_0 = 0.5$, $H = 100$ km/s Mpc). The full-drawn line corresponds to a flux density of 8 mf.u.

may be noted that especially for low redshift objects (for which the emission frequency is also low) the detection limit puts extremely low limits on the radio luminosity of these objects.

A discussion of the detection statistics of this QSO sample and their relevance to observations of QSS's will be given in another paper (Fanti *et al.*, 1972).

V.3. Notes on Individual Objects

AB 69 was observed in two fields (i.e. in fields 4 and 5); in both fields there was a small signal at the source position (map flux 3 mf.u. for both fields). The attenuation factors were about the same (10.2 versus 11.5). These factors are sufficiently high to warrant a check on the existence of the source by re-observation.

Detection of AB 82 is uncertain and, unfortunately, not easy to confirm.

For AB 99, which is equally uncertain, confirmation should be easier, as the attenuation factor here was 7.89.

The detection of AB 100 should be slightly more reliable, as the zero level around the source position is slightly depressed; the map intensity therefore may be slightly underestimated.

VI. Source Counts

As has been mentioned before, the primary motive for the present survey was the detection of QSO's rather

Table 5

NAME	RA(1950)	DEC(1950)	S MFU	Δ S	ATTEN	Z	ν_{EM}	LOG P_{EM}	REMARKS
AB 4	12 44 28.74	38 06 21.8	< 11.9		2.99				
AB 5	12 44 48.53	37 23 25.4	< 6.8		2.71				
AB 7	12 45 03.20	34 31 31.5	< 4.8		1.94	2.070	4344	< 25.07	
AB 9	12 46 28.74	37 46 49.7	< 4.7		1.89	1.241	3171	< 24.70	
AB 10	12 46 28.92	33 34 12.3	< 16.1		5.36				
AB 11	12 46 29.64	34 40 49.3	< 3.4		1.12	0.271	1798	< 23.37	
AB 15	12 47 18.30	35 05 48.7	< 11.6		4.63				
AB 16	12 47 31.85	34 56 22.8	< 7.1		2.84				
AB 17	12 48 17.68	33 47 11.3	< 4.1		1.03	0.186	1678	< 23.15	
AB 29	12 49 40.64	33 54 46.5	< 5.6		1.88	1.430	3438	< 24.88	
AB 32	12 50 33.54	33 32 13.2	< 19.2		6.40				
AB 39	12 51 41.48	35 23 09.1	< 15.0		6.00				
AB 43	12 52 20.74	35 32 46.4	< 8.2		2.06				
AB 44	12 52 24.56	36 58 52.6	< 17.8		5.93				
AB 46	12 52 52.73	35 28 27.3	< 4.0		1.98				
AB 47	12 52 57.94	35 55 24.2	< 3.4		1.35	0.221	1727	< 23.20	
AB 48	12 52 59.06	35 39 57.1	< 2.9		1.15				
AB 49	12 53 05.71	37 08 11.8	< 5.5		1.83				
AB 50	12 53 18.83	37 13 25.0	< 6.0		1.49				
AB 51	12 53 22.91	35 12 43.0	< 3.0		1.51				
AB 53	12 53 30.31	37 22 12.5	< 5.7		1.63				
AB 54	12 53 38.56	35 48 42.5	< 2.1		1.04				
AB 58	12 54 29.13	35 55 23.0	< 7.4		1.65				
AB 59	12 54 34.20	36 49 13.8	< 9.3		3.09				
AB 60	12 54 43.10	37 30 21.7	< 6.9		1.98				
AB 61	12 54 47.38	35 38 36.0	< 2.7		1.79				
AB 62	12 54 54.99	37 03 27.4	67.5	3.1	1.22	0.280	1811	24.70	0.09P 0.1N
AB 64	12 55 02.14	35 21 20.6	< 3.5		1.41	0.183	1673	< 23.07	
AB 67	12 55 40.26	37 15 17.4	< 6.0		1.50	1.530	3579	< 24.96	
AB 68	12 55 56.72	36 44 22.8	< 26.1		7.47				
AB 69	12 56 07.84	35 44 53.7	33.3	20.5	10.24	1.864	4052	25.84	POSSIBLE DETECTION
AB 70	12 56 18.40	37 23 43.6	< 13.2		3.77				
AB 73	12 56 29.62	36 39 35.3	< 13.1		4.37				
AB 75	12 56 51.11	36 48 07.6	< 8.1		2.02	2.075	4351	< 25.29	
AB 76	12 57 02.52	36 35 34.9	< 8.2		3.28				
AB 78	12 57 26.68	34 39 31.4	15.8	3.8	3.07	1.375	3360	25.30	
AB 79	12 57 40.89	35 06 51.7	< 18.6		4.35				
AB 82	12 58 02.89	37 12 40.0	7.2	4.8	2.41				POSSIBLE DETECTION
AB 83	12 58 29.96	36 51 32.5	< 3.5		1.01				
AB 84	12 58 31.36	34 04 43.1	< 4.2		1.69	0.690	2391	< 24.21	
AB 85	12 58 41.85	34 27 45.4	< 3.9		1.12				
AB 86	12 58 41.74	35 38 44.0	< 4.0		1.35	0.320	1867	< 23.59	
AB 87	12 58 49.50	34 22 38.1	< 3.2		1.05	0.780	2518	< 24.18	
AB 88	12 59 13.16	37 12 32.9	< 7.7		3.08				
AB 89	12 59 20.88	36 46 01.8	< 3.7		1.47	1.200	3112	< 24.57	
AB 90	12 59 30.92	34 27 08.8	< 5.9		1.47	1.956	4182	< 25.12	
AB 91	12 59 32.05	32 21 54.7	< 6.3		2.09	0.095	1549	< 22.76	
AB 93	12 59 48.76	37 00 17.4	< 8.8		2.21				
AB 94	12 59 51.88	35 07 40.8	< 7.0		2.82				
AB 97	13 00 18.05	35 18 12.3	< 5.0		1.98				

Table 5 (continued)

NAME	RA(1950)	DEC(1950)	S MFU	Δ S	ATTEN	Z	ν_{EM}	LOG P_{EM}	REMARKS
AB 98	13 00 22.97	38 02 55.4	< 11.9		4.76				
AB 99	13 00 29.41	38 08 02.9	23.7	15.8	7.89				POSSIBLE DETECTION
AB 100	13 00 42.51	36 07 33.5	6.2	4.4	2.08	0.060	1499	22.37	POSSIBLE DETECTION
AB 101	13 00 50.49	32 35 16.2	< 4.8		1.37				
AB 102	13 00 51.62	35 09 56.6	< 23.9		5.94				
AB 103	13 00 56.16	37 20 12.7	< 6.2		3.12				
AB 104	13 01 08.25	32 23 33.3	< 3.5		1.01				
AB 106	13 01 34.60	37 30 06.9	< 4.5		1.29	0.040	1471	< 21.87	
AB 109	13 01 41.98	35 49 21.6	< 3.6		1.03	0.330	1881	< 23.56	
AB 110	13 01 51.54	37 49 50.5	< 2.8		1.18				
AB 111	13 01 53.01	37 34 50.8	< 2.8		1.11				
AB 112	13 02 01.07	37 56 11.7	< 2.8		1.07				STAR
AB 114	13 02 11.01	32 22 39.7	13.6	2.0	1.58				0.37F 5.8S
AB 115	13 02 17.07	35 45 11.4	< 5.0		1.26	1.290	3240	< 24.76	
AB 119	13 03 02.70	37 43 21.2	< 4.4		1.74				
AB 120	13 03 13.17	37 37 22.4	< 5.3		2.12				
AB 121	13 03 21.49	32 37 42.4	< 30.2		12.07				
AB 124	13 03 36.94	34 34 00.0	< 50.6		10.12				
AB 128	13 04 07.28	36 45 06.5	< 3.0		1.22				
AB 129	13 04 09.02	36 53 32.1	< 4.6		1.83				
AB 131	13 04 20.44	37 20 14.7	< 2.9		1.17				
AB 133	13 04 48.01	34 40 24.2	< 5.1		2.05	0.184	1675	< 23.23	
AB 134	13 04 52.08	37 28 38.3	< 5.2		1.05	0.450	2051	< 23.96	
AB 135	13 05 03.82	37 13 38.6	< 4.4		1.25				
AB 136	13 05 05.43	37 27 57.9	< 3.6		1.04				
AB 137	13 05 05.94	37 26 43.8	< 3.1		1.02				
AB 138	13 05 10.69	36 48 49.0	< 3.5		1.41				
AB 139	13 05 20.58	35 17 55.3	< 11.7		2.34				
AB 140	13 05 23.34	37 26 30.3	< 2.7		1.07				
AB 141	13 05 24.65	36 25 21.2	< 4.7		1.58	0.920	2716	< 24.48	
AB 142	13 05 29.33	35 17 41.1	< 6.9		2.31	0.300	1839	< 23.77	
AB 143	13 06 01.52	34 32 45.5	< 16.3		4.65				
AB 144	13 06 18.87	37 56 29.0	< 5.6		2.80				
AB 145	13 06 22.98	33 45 26.0	< 25.0		10.00				
AB 146	13 06 21.60	35 23 01.4	< 20.9		5.97				
AB 147	13 06 54.22	35 01 08.5	< 5.5		2.20	0.190	1683	< 23.29	
AB 148	13 06 55.27	34 32 51.8	< 37.4		9.35				
AB 149	13 07 04.18	35 55 32.5	< 11.4		4.54				
AB 152	13 07 48.62	37 30 01.5	< 16.6		6.63				
AB 153	13 08 18.88	33 39 10.5	19.2	2.4	1.20				0.31P 6.6S
AB 154	13 08 16.63	38 12 42.1	< 4.5		1.50	2.090	4372	< 25.05	POSSIBLY EQUAL DOUBLE S_{TOTAL}= 13.4±7.4
AB 155	13 08 23.40	33 57 43.7	< 4.6		1.54				
AB 160	13 08 47.03	33 12 49.1	< 25.2		10.10				
AB 161	13 08 55.58	33 27 36.0	< 4.5		1.81				
AB 162	13 09 16.86	34 02 44.5	< 7.2		2.05	1.750	3891	< 25.13	
AB 163	13 09 13.95	37 50 03.3	< 3.2		1.60	0.540	2179	< 23.90	
AB 165	13 10 17.53	33 23 18.7	< 10.2		5.12				
AB 167	13 11 19.04	33 34 39.4	< 22.3		8.92				
AB 168	13 11 19.51	36 15 40.7	< 18.5		7.41	2.084	4363	< 25.66	

than the determination of source counts. We nevertheless derived preliminary counts in the flux density range 9–720 mf.u. since at 1400 MHz very little information is available as yet below some tenths of a flux unit.

A synthesis telescope like the WSRT measures the sky brightness distribution, multiplied by the reception pattern of the individual antennae. As a result, the completeness of a sample of sources observed with such a telescope decreases strongly with decreasing flux density (i.e. the search area is smaller for the weaker sources). One may however define complete samples with respect to map flux (i.e. attenuated real-sky flux density). For the present observations we could define complete samples in this sense down to map fluxes between 6.75 and 10.0 mf.u. Because of this variation in limiting map flux we derived source counts for each field in the following way.

For every individual source with a map flux larger than the limiting map flux of the field in which it was detected, we determined the distance to the field center where the map flux would have become equal to the limiting map flux. From this distance we computed the area over which the source would have been included in the complete sample; i.e. the area over which it would have been observable. Because the complete samples contained only sources within a distance of 0.7 degrees from the respective field centers, the maximum area over which a source can have been observable is 1.54 square degrees. The inverse of the area so computed gives the number of sources per steradian of a particular flux density, as implied by the detection of this single source. Sources that were detected in two fields (due to partial overlap of the fields) were considered to have been observable once over half the total area taking proper account of the region of overlap. Extended sources were treated like unresolved sources, but the peak flux density was used rather than the integrated flux density to determine the contribution to the counts. The five complexes where we could derive source parameters for the individual components were treated as single sources with a flux density equal to the sum of the peak flux densities of the components.

The counts resulting from this procedure, averaged over the eighteen fields, are given in Table 6 in the form of dN/dS in flux density intervals $9\times(1.55)^{n-1}$ to $9\times(1.55)^{n}$ mf.u., where $n=1-10$. S^{*} is the weighted mean flux density of the sources in a certain flux density interval. It should be realized that the counts have not been corrected for random errors in flux density nor for possible systematic errors in the attenuation factors (cf. Section II.4). The quoted errors in dN/dS (in brackets) are consequently merely formal sample size errors. The last two columns of Table 6 contain two sets of integral counts, both of which are based on $N(S=0.465\text{ f.u.})=500\text{ sterad}^{-1}$, as extrapolated from the 1400 MHz counts published by Bridle *et al.* (1972). The two sets derive from different values for dN/dS (given in parentheses) in the interval 124–465 mf.u., the reason for which is explained below.

It obviously is interesting to compare the present results with counts at higher flux density levels. Two extensive surveys exist at 1400 MHz, viz. the Green Bank/Owens Valley survey (Bridle *et al.*, 1972) and the Ohio survey (Harris and Kraus, 1970; Kraus, 1972). Since, as Jauncey and Niell (1971) pointed out, the Ohio observations are beset with rather large systematic errors below one flux unit, we restrict our discussion to a comparison with the "Green Bank" data. Figure 6 shows the Green Bank and WSRT data, both normalized with respect to counts in a hypothetical non-expanding non-evolving Euclidean Universe. It is immediately apparent that around 450 mf.u. a rather large discrepancy exists between the two sets of data: above 0.2 f.u. we have detected 25 sources whereas only 13 sources are expected on the basis of an extrapolation of the Green Bank counts.

Two possible explanation for the observed discrepancy were considered. Firstly, unexpectedly large systematic errors may exist in our data above, say, 0.1 f.u. The WSRT data below this level seem to be in good agreement with an extrapolation of the Green Bank counts to flux densities below 0.5 f.u. (the open circles in Fig. 6 represent a possible interpolation between the respective counts, upon which the alternative integral counts in Table 6 are based). Secondly, the excess of

Table 6. 1415 MHz source counts

S (mf.u.)	n	S^{*} (mf.u.)	dN/dS (sterad^{-1} f.u.$^{-1}$)	$N(S)$ (sterad^{-1})	
9.0				$6.95\,10^{4}$	$6.70\,10^{4}$
	21	11.8	$4.22(0.92)\,10^{6}$		
14.0				$4.86\,10^{4}$	$4.61\,10^{4}$
	32	17.5	$2.73(0.48)\,10^{6}$		
21.6				$2.77\,10^{4}$	$2.52\,10^{4}$
	19	26.9	$5.70(1.31)\,10^{5}$		
33.5				$2.09\,10^{4}$	$1.84\,10^{4}$
	25	42.0	$3.97(0.79)\,10^{5}$		
52.0				$1.36\,10^{4}$	$1.11\,10^{4}$
	21	67.1	$1.65(0.36)\,10^{5}$		
80.5				$8.88\,10^{3}$	$6.43\,10^{3}$
	13	103	$6.14(1.70)\,10^{4}$		
124				$6.16\,10^{3}$	$3.70\,10^{3}$
	15	148	$4.02(1.04)\,10^{4}$ ($2.67\,10^{4}$)		
193				$3.40\,10^{3}$	$1.87\,10^{3}$
	13	239	$2.00(0.55)\,10^{4}$ ($0.91\,10^{4}$)		
300				$1.29\,10^{3}$	$9.04\,10^{2}$
	6	405	$4.80(1.96)\,10^{3}$ ($2.45\,10^{3}$)		
465				$5.00\,10^{2}$	
	6	562	$3.09(1.26)\,10^{3}$		
720					

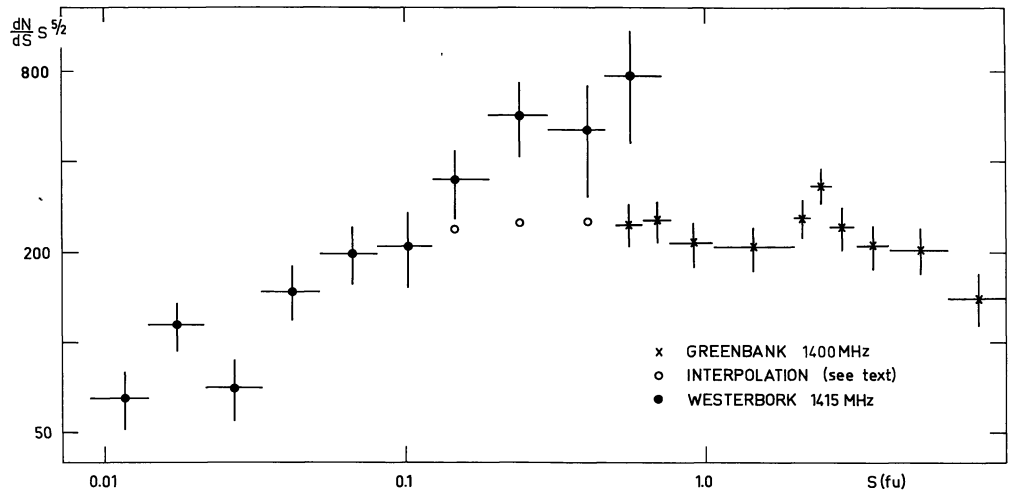

Fig. 6. The "normalized" differential counts from the present data together with those from Green Bank 1400 MHz data

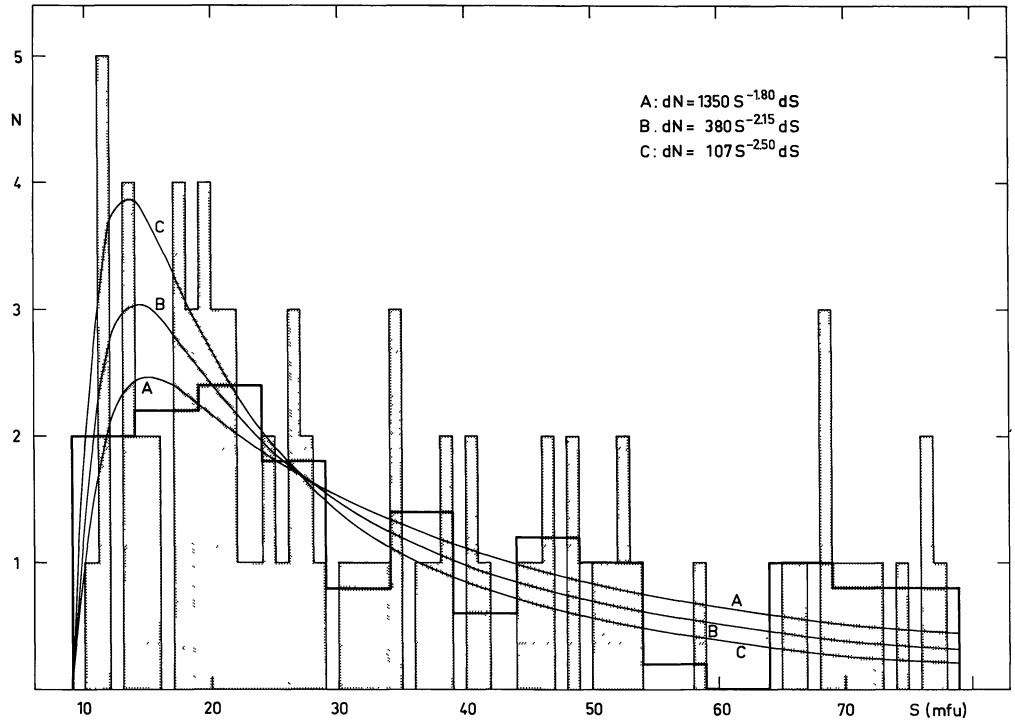

Fig. 7. The apparent distribution with respect to flux density of a complete sample of sources with $S < 80$ mf.u. Three predictions of the same distribution, which are characterized by different slopes, are drawn in for comparison. The model distributions have been normalized to the number of sources observed between 9 and 79 mf.u.

sources above 0.1 f.u. may be real, i.e. it is an intrinsic property of the survey region.

As for the first explanation, we roughly estimated the magnitude of possible systematic errors and found that these most probably do not exceed the statistical uncertainties in dN/dS above 0.1 f.u. Assuming therefore that the observed excess is at least partly due to an intrinsic excess of sources, we investigated whether it can have been caused by selection effects or whether it should be attributed to an anisotropic distribution of the relatively stronger radio sources. The particular arrangement of the eighteen fields might for example be responsible for such a selection effect, because we tried to observe as many QSO's as possible. In order to investigate this question we computed two sets of counts, one for the nine fields with a QSO surface density below average (fields 1, 2, 3, 9, 10, 11, 13, 16, 18), another for the remaining nine fields. There is a contrast in QSO surface density between the two groups of about a factor of two. To within the statistical uncertainties there appears to be no correlation between the surface density of QSO's and that of radio sources

above 0.1 f.u. For sources below 0.1 f.u. we did not investigate a possible correlation of this kind. We are therefore led to tentatively conclude that the relatively stronger radio sources appear to cluster on scales of the order of about ten squares degrees. Although the evidence for such clustering is as yet not very strong, there are other observations which strengthen the above conclusion. Firstly, in another survey with the WSRT ($\alpha \sim 1^h$, $\delta \sim 30°$) the surface density of sources above 0.1 f.u. seems to be definitely lower than in the present survey. Secondly, recent observations by Maslowski (1971, 1972) with the Green Bank 300-foot telescope indicate a marginally significant difference between the counts in the 5 C 1 and 5 C 2 regions around ~ 0.3 f.u. Further observations have of course to be made to investigate this interesting effect in more detail. It is especially of interest to try and optically identify those sources that cause the observed excess. Moreover, observations at different frequencies are needed in order to understand the negative results of attempts to detect clustering at frequencies below 1400 MHz.

An important datum to be derived from the present observations is the slope of the counts at the lowest flux densities observed. To the data in Table 6 we fitted a power law ($dN = AS^{-k}\,dS$) in the flux density range 9–80 mf.u. (the total number of sources in this range is 131). We find: $k = 1.9$. and $A = 900$ sterad^{-1} f.u.$^{-1}$. In order to minimize possible effects of incompleteness at the lowest flux densities we also analyzed the data in the following way. Only those 14 fields were considered for which the limiting map flux was equal to or smaller than 9 mf.u. In these fields we defined samples complete to a map flux of 9 mf.u. (As before, the peak value was used for extended sources.) The so defined complete sample consists of 81 sources between 9 and 79 mf.u. The distribution of these 81 sources over flux density is given in Fig. 7 where N is the number of sources per mf.u. interval. The heavily drawn distribution represents averages over 5 mf.u. intervals. The curves labeled A to C are predictions of the same distribution for different values of k. These theoretical curves have been normalized so as to make the total number of sources between 9 and 79 mf.u. in each case equal to 81.

It is immediately clear that a value for k of 2.5 may be excluded on the basis of the present observations. In order to decide between the possibilities A and B we performed two χ^2-tests with different sampling intervals. Although the statistics are not very good, curve A seems to give a marginally better fit than curve B if we consider the complete flux density range. Between 19 and 69 mf.u. curve B is slightly better than curve A. We therefore conclude that the value for k between 9 and 79 mf.u. is most probably in the range from 1.8–2.1. It should be mentioned that the deep Cambridge surveys yielded a value for k of 1.8 at slightly higher source densities (e.g. Ryle, 1968).

Acknowledgements. The authors want to thank the staff of the Westerbork Radio Observatory for doing the observations, Dr. W. N. Brouw and Mr. T. Hoekema for providing the computer programs without which the reduction and analysis would have been impossible, Messrs. J. W. Brotherhood and H. W. van Someren Gréve for their assistance in the reduction and Mr. J. F. Planken for the photographic reproductions.

Thanks are also due to Dr. A. Braccesi for making available the four colour Palomar Schmidt plates and time at the Bologna measuring machine, as well as providing magnitudes for some of the identifications. One of us (J.K.K.-M.) gratefully acknowledges the hospitality of the members of the radio astronomy group at Bologna.

The Westerbork Radio Observatory is operated by the Netherlands Foundation for Radio Astronomy with the financial support of the Netherlands Organization for the Advancement of Pure Research (Z.W.O.).

References

Anderson, B., Donaldson, W. 1967, *Monthly Notices Roy. Astron. Soc.* **137**, 81.
Braccesi, A., Formiggini, L., Gandolfi, E. 1970, *Astron. & Astrophys.* **5**, 264.
Braccesi, A., Lynds, C. R., Sandage, A. 1968 *Astrophys. J.* **152**, L 105.
Bridle, A. H., Davis, M. M., Fomalont, E. B., Lequeux, J. 1972, *Nature Phys. Sc.* **235**, 123.
Brouw, W. N. 1971, Data Processing for the Westerbork Synthesis Radio Telescope, Ph. D. Thesis, Leiden.
Fanti, R., Formiggini, L., Lari, C., Padrielli, L., Katgert-Merkelijn, J. K., Katgert, P. 1972, *Astron. & Astrophys.* in press.
Harris, B. J., Kraus, J. D. 1970, *Nature* **227**, 785.
Jauncey, D. L., Niell, A. E. 1971, *Nature Phys. Sc.* **229**, 223.
Kraus, J. D. 1972, *Nature Phys. Sc.* **236**, 4.
Maslovski, J. 1971, *Astron. & Astrophys.* **14**, 215.
Maslowski, J. 1972, *Astron. & Astrophys.* **16**, 197.
Ryle, M. 1968, *Ann. Rev. Astron. Astrophys.* **6**, 249.
Schmidt, M. 1970, *Astrophys. J.* **162**, 371.

P. Katgert
J. K. Katgert-Merkelijn
R. S. Le Poole
H. van der Laan
Sterrewacht
Leiden, Netherlands